Discovery of the new isotope ^{251}Lr: the impact of the hexacontetrapole deformation on single-proton orbital energies near the Z=100 deformed shell gap

T. Huang,[1, 2] D. Seweryniak,[2, *] B. B. Back,[2] P. Bender,[3] M. P. Carpenter,[2] P. Chowdhury,[3] R. M. Clark,[4] P. Copp,[2] X.-T. He,[5] R. D. Herzberg,[6] D. Hoff,[3] H. Jayatissa,[2] T. L. Khoo,[2] F. G. Kondev,[2] G. Morgan,[7] Ch. Morse,[4] A. Korichi,[8] T. Lauritsen,[2] C. Müller-Gatermann,[2] D. Potterveld,[2] W. Reviol,[2] A. Rogers,[3] S. Saha,[3] G. Savard,[2] K. Sharma,[3] S. Stolze,[2] S. Waniganeththi,[3] G. Wilson,[2] J. Wu,[2] Y.-F. Xu,[5] and S. Zhu[9, †]

[1]*Institute of Modern Physics, Chinese Academy of Sciences, Lanzhou 730000, China*
[2]*Argonne National Laboratory, Argonne, IL 60439, USA*
[3]*University of Massachusetts, Lowell, MA 01854, USA*
[4]*Lawrence Berkeley National Laboratory, Berkeley, CA 94720, USA*
[5]*College of Materials Science and Technology, Nanjing University of Aeronautics and Astronautics, Nanjing 210016, China*
[6]*University of Liverpool, Liverpool, UK*
[7]*Louisiana State University, Baton Rouge, LA 70803, USA*
[8]*IJCLab, IN2P3-CNRS, France*
[9]*Brookhaven National Laboratory, Upton, NY 11973, USA*
(Dated: November 10, 2022)

The products of the ^{203,205}Tl(^{50}Ti,2n) fusion-evaporation reactions were studied using the recently commissioned Argonne Gas-Filled Analyzer (AGFA) at Argonne National Laboratory. Two α-decay activities with energies of 9210(19) and 9246(19) keV and the half-lives of 42^{+42}_{-14} ms and $24.4^{+7.0}_{-4.5}$ ms were observed which were followed by the known α decays of ^{247}Md and ^{243}Es. They are interpreted as originating from the $1/2^-$[521] and $7/2^-$[514] single-proton Nilsson states in the hitherto unknown isotope ^{251}Lr. From the measured Q$_\alpha$ values the $1/2^-$ level was placed 117(27) keV above the $7/2^-$ level in ^{251}Lr in contrast to ^{255}Lr where the $1/2^-$ level is the lowest. Also, the α decay of ^{253}Lr was studied in more detail and a new α line at 8660(20) keV was found and a new half-life value of 2.46(32) s for an isomeric state in ^{253}Lr was measured. The ^{251,253,255}Lr Q$_\alpha$ values were compared with predictions of various mass models. The relative energies of the $1/2^-$[521] and $7/2^-$[514] single-proton Nilsson states in ^{251,253,255}Lr isotopes were compared with results of the Cranking Shell Model (CSM) with pairing treated using the particle-number-conserving (PNC) method. The level separation and in particlular the level order change between ^{251}Lr and ^{255}Lr was reproduced only when the hexacontetrapole deformation ε_6 was included in the calculations.

Introduction. The discovery of a new isotope, and identifying its associated decay modes, is the first step toward understanding nuclear structure at the extremes of stability. This is a central theme in contemporary nuclear physics. For heavy nuclei above Uranium (Z=92) the favored approach for creation of new isotopes is to use intense (microampere) heavy-ion beams of stable ions which undergo fusion-evaporation reactions on nuclei of various target materials. The low production cross-sections (typically less than a few nanobarns) means that such experiments require powerful magnetic separators and very sensitive detection techniques in order to identify and study the handful (down to the level of only one or two new atoms in an experiment). First and foremost, many new isotopes were discovered during the studies of the new Superheavy Elements [1–3]. Recent examples include the discovery of new isotopes of U and Np (Z=92 and 93, respectively) [4, 5], new isotopes of Bk (Z=97) and Es (Z=99) [6], and the recent claim and counterclaim of the discovery of ^{244}Md (Z=101) [7, 8].

While finding a new isotope is exciting, there are often compelling reasons to study the decay and structure of such nuclei. In the examples mentioned above, the evolution of alpha-decay properties in the light U-Np isotopes is shedding light on the alpha formation process while the new odd-odd Bk, Es, and Md isotopes can undergo electron capture and the delayed fission of the decay daughters provides a new probe of the low-energy spontaneous fission process. Here, we described the discovery of the new isotope ^{251}Lr and a study of the structure and decay of this new isotope and its previously known odd-neighbor ^{253}Lr. With Z=103, these odd-proton isotopes offer a compelling opportunity to understand the structure of the Superheavy Elements. In particular, the proton $1/2^-$[521] Nilsson orbital, which originates from the $f_{5/2}$ spherical orbital located just above the spherical Z=114 gap [9], can be found near the ground state in Md, Lr and Db proton-rich isotopes. However, the relative energy of this orbital is only available in ^{255}Lr and its α-decay daughter ^{251}Md [10].

^{253}Lr was observed for the first time following the α decay of ^{257}Db [11]. Later, more statistics were obtained in Ref. [12]. More recently, it was produced directly using the ^{209}Bi(^{48}Ca,4n)^{253}Lr reaction [13]. Its α decay properties were also reported when it was observed as part of the ^{261}Bh α-decay chain [14]. So far, only two α lines were assigned to ^{253}Lr, which were tentatively interpreted as the decay of the excited $1/2^-$[521] state and the $7/2^-$[514] ground state, respectively. These data were not enough to deduce the excitation energy of the

1/2$^-$[521] state in ^{253}Lr. To understand the single-proton orbital evolution in Lr isotopes, the detailed knowledge of the alpha-decay fine structure in ^{253}Lr is required. The decay of even lighter isotope ^{251}Lr has not been firmly determined. Only in Ref. [15], a spontaneous fission observed 39 ms after a single candidate for an unknown ^{255}Db α decay was tentatively assigned to the decay of the daughter ^{251}Lr nucleus. No correlations with known decays were reported in this case.

This paper reports the discovery of ^{251}Lr and the first observation of its α decay. Also, the α-decay fine structure studies of ^{253}Lr was studied in more detail. The experimental setup and the experimental results are described below followed by a discussion of the α-decay Q-values and the single-proton orbital evolution in proton-rich odd-mass Lr isotopes.

Experimental details and results. ^{251,253}Lr nuclei were synthesized using the ^{203,205}Tl(^{50}Ti,2n) fusion-evaporation reactions, respectively. The ^{50}Ti beam with an energy of 237 MeV and an average beam intensity of 70 pnA was delivered by the ATLAS linear accelerator at the Argonne National Laboratory. The targets were composed of a 0.5 mg/cm^2-thick Tl layer which was sandwiched between carbon layers to improve radiative cooling and prevent sputtering of the target material. The thickness of the entrance and exit carbon layers was 40 μg/cm^2 and 10 μg/cm^2, respectively. The enrichment was 97.2 % and 99.82% for the ^{203}Tl and ^{205}Tl targets, respectively. Sixteen targets were mounted on a target wheel with 15 cm radius. The wheel rotation frequency was about 1200 rpm and the beam was swept away to avoid hitting the target wheel spokes. The ^{251,253}Lr nuclei were produced during an irradiation time of $\simeq$ 49 hours and $\simeq$ 66 hours, respectively. The recoiling reaction products were separated from the beam in the Argonne Gas-Filled Analyzer (AGFA) and then passed through a parallel grid avalanche counter (PGAC) before they were implanted into a 300 μm-thick 64x64 mm^2 Double-sided Si Strip Detector (DSSD). The front and back side of the DSSD were divided into 160 strips each, which were mutually orthogonal, resulting in 25600 pixels. The implant and subsequent α-decay energies were measured in the same pixel. The decay times were determined by temporal and spatial correlations between implants and decays. An array of eight 4x7cm^2 300 μm-thick Single-sided Si Strip Detectors (SSSD), which formed a tunnel, was mounted in front of the DSSD. They were used to catch α particles escaping from the DSSD. To veto energetic light particles like protons and He ions, a 300 μm-thick 5x5 cm^2 Si detector, was placed behind the DSSD. The ^{208}Pb(^{48}Ca,2n) reaction was used to implant well-known α radioactivities ^{254}No, ^{250}Fm, and ^{246}Cf to calibrate the DSSD and the SSSD.

Implanted recoiling fusion-evaporation products with energies between 10 MeV and 30 MeV were selected using the time of flight between the PGAC and the DSSD.
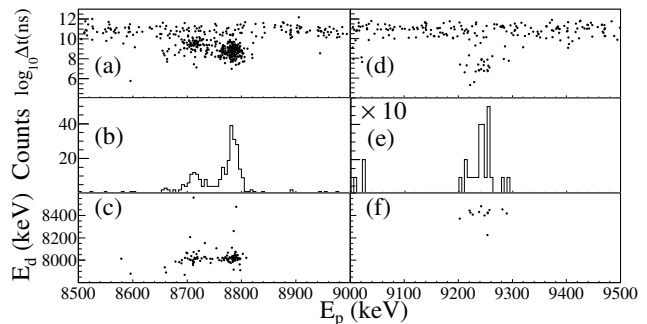

FIG. 1. (a) The decay energy versus the logarithm base 10 of the time difference between an implantation and a subsequent decay expressed in ns for the ^{50}Ti + ^{205}Tl reaction, (b) the ^{253}Lr decay energy spectrum corresponding to the decay time window of 16 s, (c) the α decay correlations between ^{253}Lr and its daughter nucleus ^{249}Md for daughter decay times less than 160 s (the daughter α-decay energy is the sum of energies deposited in the SSSD and the DSSD), (d) same as (a) for the ^{50}Ti + ^{203}Tl reaction, (e) the ^{251}Lr decay energy spectrum corresponding to the time window of 0.3 s, (f) the α decay correlations between ^{251}Lr and its daughter nucleus ^{247}Md for daughter decay times less than 5 s.

Subsequently, a search for correlated α-decay chains following the recoil implants in the same DSSD pixel was performed. The identification plots for ^{253}Lr and ^{251}Lr decays are displayed in Fig. 1 and Fig. 2. Because of their relatively short lifetime and low implantation rates in the DSSD, the decays of these two isotopes could be clearly separated from random background events in the two-dimensional histograms containing the α-decay energy as a function the logarithm of the decay time, as shown in Fig. 1(a) and (d), respectively. Fig. 1(b) and (e) show the corresponding α-decay energy spectra with the decay times shorter than 16 s and 0.3 s, respectively. The correlations between the mother and the daughter α particles are displayed in Fig.1(c) and (f), with the daughter decay time shorter than 160 s and 5 s, respectively. Because of the small energy differences between the observed α-particle lines in ^{253}Lr and ^{251}Lr, the escaping α particles were included only for the daughter nuclei by summing the energies deposited in the DSSD and the SSSD. The correlations for the daughter and the granddaughter α particles with no additional decay time conditions are shown in Fig. 2. Based on these correlations, ^{253}Lr and ^{251}Lr α lines were unambiguously assigned based on the well known α-decay properties of ^{249}Md, ^{247}Es and ^{247}Md, ^{245}Es, respectively.

The α-decay properties determined in the present work are summarized and compared with the literature values in Table. I. Following the ^{50}Ti + ^{205}Tl reaction, 275 full-energy ^{253}Lr α decays were observed. As can be seen in Fig. 1(b), three α lines were proposed in ^{253}Lr with energies of 8785(14), 8715(14) and 8660(20) keV and half-lives of 0.65(5), 2.46(32) and 0.43$^{+0.23}_{-0.11}$ s, respectively.
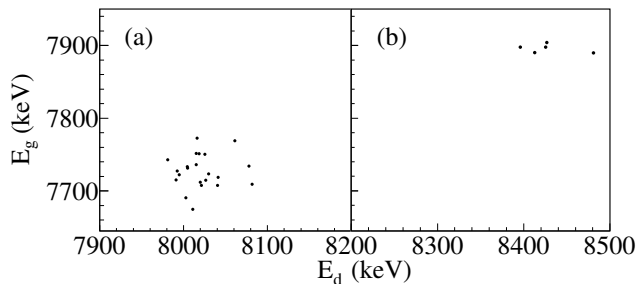
FIG. 2. α-decay correlations between daughter and grand daughter nuclei following (a) the ^{205}Tl(^{50}Ti,2n)^{253}Lr and (b) the ^{203}Tl(^{50}Ti,2n)^{251}Lr reaction. The decay time windows are the same as in in Fig.1 (c) and (d), respectively.

The α-decay line at 8660 keV was observed for the first time. It is correlated with 3 α-decay events with energies of 7985, 7939 and 7891 keV, which were attributed to the α decays of ^{249}Md, as shown in Fig.2(c). The last two energies are the result of summing of energies deposited in the DSSD and the SSSD which explains their slightly lower energies due to energy loses in the detector dead layers. The half-life corresponding to the 3 daughter events is 27^{+37}_{-10} s which is consistent with the half-life of 23(3)s for ^{249}Md [13]. Following the ^{50}Ti + ^{203}Tl reaction, 24 events distributed among 2 full-energy α-decay peaks were assigned to the new isotope ^{251}Lr, as shown in Fig.1(e). The α energies of 9246(19) and 9210(19) keV and half-lives of $24.4^{+7.0}_{-4.5}$ and 42^{+42}_{-14} ms were deduced for these 2 lines, respectively. The deduced half-lives of α decays following the 9246 keV and 9210 keV α decays are $1.20^{+0.52}_{-0.28}$ s and $0.72^{+0.98}_{-0.26}$ s, respectively, and their energy of 8430(13) keV are consistent with the half-life of 1.21(12) s and the α energy of 8421 keV for the strongest ground-state α-decay branch in ^{247}Md measured in Ref. [16]. Assuming an estimated transmission efficiency of 50% for AGFA, the production cross sections for ^{253,251}Lr were determined to be about 7 nb and 800 pb, respectively.

Discussion. In the proton-rich Md and Lr isotopes near the N =152 neutron closed shell, the proton $1/2^-[521]$ and $7/2^-[514]$ Nilsson levels form a doublet close to the Fermi surface and were proposed as the ground state or the first excited state in these nuclei. One of these states is isomeric because of the M3 multipolarity of the electromagnetic transition between these two states. The α decays between Lr and Md isotopes connect primarily levels with the same spin and parity. However, data for these isotopes are scarce and the isomer excitation energies were deduced only in ^{255}Lr and ^{251}Md based on the α-decay fine structure observed in ^{255}Lr [10].

The proposed decay level schemes for ^{251}Lr and ^{253}Lr are compared to ^{255}Lr [12] in Fig. 4. The properties of the 3 α lines attributed to ^{253}Lr are shown in Table. I. The energy of 8785 keV and the half-life of 0.65 s of
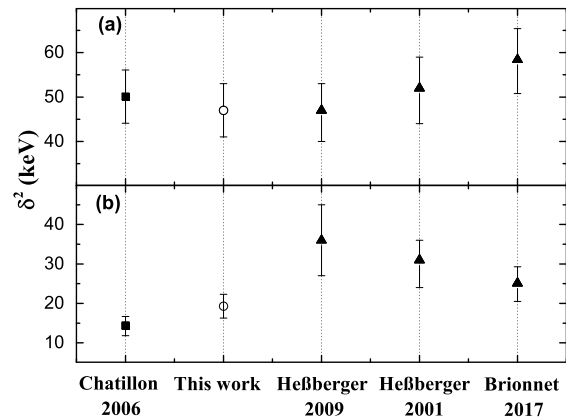

FIG. 3. Comparison of the α-decay reduced widths in ^{253}Lr (solid triangles, open circle) and ^{255}Lr (solid squares) for (a) the 8785 keV and the 8457 keV α line and for (b) the 8715 keV and the 8365 keV α line, obtained in [10], this work, [13], [12], and [17].

the strongest line are consistent with the previous studies [12]. Fig. 3 (a) shows the α-decay reduced width deduced for this α line in comparison with that of the 8457 keV α line in ^{255}Lr corresponding to the α decay of the $7/2^-$ isomer [10]. The $7/2^-$ isomer in ^{255}Lr is the most strongly populated α decaying state although it partially decays to the ground state. Similar values of the reduced widths indicate that the 8785 keV line corresponds to the decay of the $7/2^-$ level in ^{253}Lr. The energy of the 8715 keV line is close to the previously measured value, while the half-life measured in this work marginally disagrees with the previously measured values, $1.49(^{+0.3}_{-0.21})s$ [12] and $1.60(^{+0.24}_{-0.18})s$ [20], but is consistent with the recently measured value of $2.00^{+0.16}_{-0.19}s$ [17]. The α-decay reduced width for this transition is compared to that of the 8365 keV decay from the $1/2^-$ ground state in ^{255}Lr in Fig.3 (b). The value deduced from this work is much closer to the one in ^{255}Lr which suggests that the 8715 keV line deexcites the $1/2^-$ level in ^{253}Lr. The 8660 keV line was observed for the first time in this work and its half-life is consistent with that of the 8785 keV transition. Thus, it is proposed to originate from the same level. Its energy indicates that it decays to an excited state at about 127 keV in ^{249}Md. A weak 8420 keV line in ^{255}Lr depopulating the $7/2^-$ level was proposed to populate the $11/2^-$ member of the $7/2^-[514]$ rotational band at 135 keV in ^{251}Md. The α-decay reduced width for the 8660 keV transition is similar to that of the 8420 keV $7/2^--11/2^-$ decay in ^{255}Lr suggesting a similar interpretation. The α particles feeding the $11/2^-$ level are subject to summing with the conversion electrons, X rays and Auger electrons corresponding to the successive $11/2^--9/2^-$ and
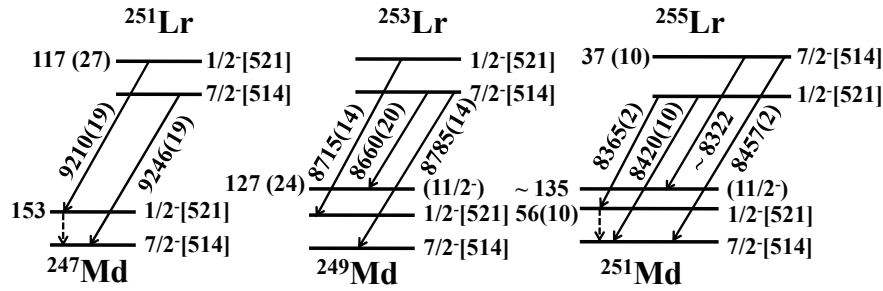
^{251}Lr ^{253}Lr ^{255}Lr

117 (27) —— 1/2⁻[521] —— 1/2⁻[521] 37 (10) —— 7/2⁻[514]
      —— 7/2⁻[514] —— 7/2⁻[514] —— 1/2⁻[521]

9210(19) 9246(19) 8715(14) 8660(20) 8785(14) 8365(2) 8420(10) ~8322 8457(2)

127 (24) —— (11/2⁻) ~ 135 —— (11/2⁻)
153 ┆ —— 1/2⁻[521] —— 1/2⁻[521] 56(10) ┆ —— 1/2⁻[521]
   —— 7/2⁻[514] —— 7/2⁻[514] —— 7/2⁻[514]

^{247}Md ^{249}Md ^{251}Md

FIG. 4. Comparison of the ^{251,253}Lr level schemes deduced in this work with the ^{255}Lr level scheme from Ref. [10].

TABLE I. Alpha-decay properties of ^{251}Lr and ^{253}Lr determined in this work compared with the literature values. The α-decay widths δ^2 were deduced using the Rasmussen's method [18]. The present experiment was not sensitive to spontaneous fission and a possible small spontanous fission branch was not taken into account in the calculations.

Isotope	Production	E_α(keV)	Q_α(keV)	$T_{1/2}$	Intensity(%)	δ^2(keV)[a]	$I_i^\pi \to I_f^\pi$
^{251}Lr	^{203}Tl(^{50}Ti,2n)^{251}Lr	9246 (19)	9438 (19)	$24.4^{+7.0}_{-4.5}$ ms	83 (25)	64^{+14}_{-20}	$7/2^- \to 7/2^-$
this work		9210 (19)	9402 (19)	42^{+42}_{-14} ms	16 (9)	47^{+17}_{-47}	$1/2^- \to 1/2^-$
^{253}Lr	^{205}Tl(^{50}Ti,2n)^{253}Lr	8785 (14)	8969 (14)	0.65 (5) s	70 (7)	$46.6^{+5.6}_{-5.9}$	$7/2^- \to 7/2^-$
this work		8660 (20)	8842 (20)	$0.43^{+0.23}_{-0.11}$ s	3 (1)	$7.6^{+2.2}_{-2.3}$	$7/2^- \to (11/2^-)$[d]
		8715 (14)	8897 (14)	2.46 (32) s	27 (3)	$19.3^{+3.5}_{-3.1}$	$1/2^- \to 1/2^-$
^{253}Lr	^{209}Bi(^{48}Ca,4n)^{253}Lr	8786 (15)	8970 (15)	0.67 (6) s		$46.8^{+6.4}_{-6.7}$	$7/2^- \to 7/2^-$
[13]		8719 (15)	8901 (15)	1.32 (30) s		$35.7^{+9.1}_{-9.2}$	$1/2^- \to 1/2^-$
^{253}Lr	^{257}Db$\xrightarrow{\alpha}$^{253}Lr	8794 (10)	8978 (10)	$0.57^{+0.07}_{-0.06}$ s		$52.0^{+6.7}_{-7.6}$	
[12]		8722 (10)	8905 (10)	$1.49^{+0.3}_{-0.21}$ s		$30.8^{+5.1}_{-6.8}$	
^{253}Lr	^{257}Db$\xrightarrow{\alpha}$^{253}Lr	8788 (10)	8972 (10)	$0.520^{+0.029}_{-0.032}$ s		$58.4^{+7.0}_{-7.6}$	
[17]		8713 (10)	8896 (10)	$2.00^{+0.16}_{-0.19}$ s		$25.1^{+4.2}_{-4.6}$	
^{253}Lr	^{261}Bh$\xrightarrow{\alpha}$^{257}Db$\xrightarrow{\alpha}$^{253}Lr	8777 (20)	8960 (20)	$0.7^{+0.5}_{-0.2}$ s	53 (22)	48^{+15}_{-35}	
[14]		8710 (20)	8892 (20)	$1.2^{+0.7}_{-0.4}$ s	47 (20)	42^{+15}_{-25}	
^{255}Lr	^{209}Bi(^{48}Ca,2n)^{255}Lr	8457 (2)	8634 (2)	2.53 (13) s	26.0 (8)[g]	50.3 (66)	$7/2^- \to 7/2^-$
[10]		8420 (10)	8597 (10)	30 (4) s	≤ 3.6 (5)[f]	$5.3^{+1.2}_{-1.3}$	$1/2^- \to 7/2^-$[e]
		8420 (10)[b]	8497 (10)[c]	2.8 (6) s	2.1 (5)[g]	$16.8^{+6.1}_{-8.2}$	$7/2^- \to 11/2^-$[d]
		8365 (2)	8541 (2)	31.1 (13) s	67.1 (15)[f]	$14.4^{+2.3}_{-2.6}$	$1/2^- \to 1/2^-$

[a] all values were calculated in the present work
[b] interpreted as a result of electron summing
[c] α energy of 8322 keV was used in the calculation
[d] α angular momentum $l=2$
[e] α angular momentum $l=4$
[f] β-decay branch of 26(5)% measured in Ref.[19] was used in the calculation
[g] IT branch of 60% was used in the calculation

$9/2^-$-$7/2^-$ intra-band transitions. In the present work, events when both electrons escaped from the DSSD were observed leaving about 10 keV in the DSSD, whereas in Ref. [10] the component of the energy distribution corresponding to both electrons detected in the DSSD was reported. Alternatively, the 8660 keV line could be interpreted at the $7/2^-$-$1/2^-$ transition which would require that α particles are emitted with angular momentum $l=4$, similarly to the proposed $1/2^-$-$7/2^-$ transition in ^{255}Lr, but the reduced decay width for the 8660 keV decay is then too large to support this scenario.

The properties of the 2 α lines assigned to ^{251}Lr are shown in Table. I. The intensity ratio for the two ob-

served 9246 and 9210 keV α-decay activities is similar to that of the two strongest lines in ^{253}Lr. This indicates that they correspond to the decay of the levels with the same configurations as in ^{253}Lr, and are interpreted as the decay of the $7/2^-$ ground state and the $1/2^-$ isomeric state, respectively. No other transitions were observed in ^{251}Lr due to the low production cross section. Recently, the $1/2^-$ level was measured to be located 153 keV above the $7/2^-$ level in ^{247}Md [16]. Based of the Q_α-values for the ^{251}Lr α transitions, the $1/2^-$ level is situated 117(27) keV above the $7/2^-$ level in ^{251}Lr. Compared to ^{255}Lr, where the $7/2^-$ level is situated 37(10) keV above the $1/2^-$ level, the $1/2^-$-$7/2^-$ level order is
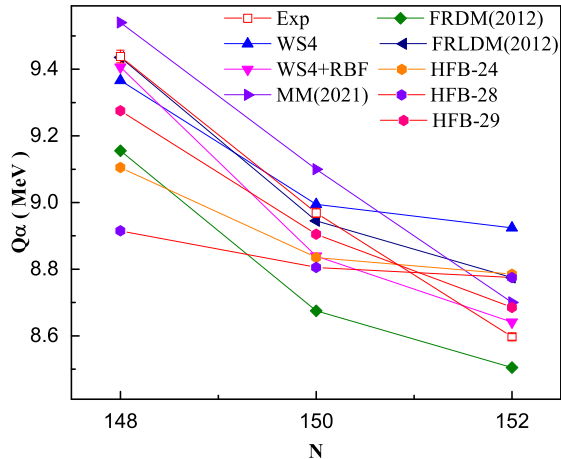
FIG. 5. The observed ground-state Q_α values for ^{251,253,255}Lr compared to the predictions of several mass models (see the text for details).

reversed (see Fig. 4).

The deduced ground-state Q_α values for ^{251,253,255}Lr can be used to test nuclear mass models. In Fig. 5, the experimental values are compared with theoretical predictions, namely, the macroscopic–microscopic models (WS4, WS4 + RBF) [21] and MM(2021) [22], the finite-range droplet/liquid-drop models (FRDM/FRLDM) [23] and the Hartree-Fock-Bogoliubov (HFB-24, HFB-28, HFB-29) model [24, 25]. All calculations reproduce the Q_α value increase towards more proton-rich Lr isotopes. The MM(2021) model reproduces the trend best but overpredicts the Q_α values by about 100 keV. The WS+RBF, FRLDM and HFB29 models agree with the data best. The ^{251}Lr Q_α value calculated using the first two models are very close to the experimental value. It is interesting to compare various interactions used in the HFB calculations. Compared to the HFB-24 interaction, the HFB-28 and HFB-29 models feature modified spin-orbit component. The HFB-29 model reproduces the data better than HFB-24 whereas for HFB-28 the agreement is worse.

Various models have been employed to calculate single-proton energies in nuclei near Z=100 and N=152. The results obtained with the macroscopic-microscopic model using the Wood-Saxon potential with the Universal set of parameters were reported in Ref. [27]. The two-center shell model was used in Ref. [28]. The calculations using the quasi-particle phonon model were presented in Ref. [29]. The predictions of the Hartree-Fock-Bogoliubov model with the Skyrme interaction were discussed in Ref. [10]. All the calculations above fail to reproduce the $1/2^-$ ground-state spin in ^{255}Lr and the change of the $1/2^-$-$7/2^-$ level order in ^{251}Lr. In Ref. [30],

the $1/2^-$[521] orbital was calculated as the ground state in ^{255}Lr after incuding the hexacontetrapole deformation. Fig. 6 shows the calculated energies of single-proton levels in ^{251,253,255}Lr using the cranked shell model (CSM) with the pairing treated using the particle-number-conserving (PNC) method. This model was used recently to describe rotational bands built on mulit-particle configurations in ^{254}No [26]. The quadrupole deformation of ε_2=0.26 was used in the calculation. The $1/2^-$-$7/2^-$ level order in Lr isotopes was successfully reproduced only when the hexacontetrapole deformation ε_6 was included. The PNC-CSM model also predicts similar ground-state and isomer configurations in ^{251}Lr and ^{253}Lr.

In summary, the new isotope, ^{251}Lr, was discovered, and its α decay was studied for the first time. The α-decay properties of ^{253}Lr were in greater detail than before. Among the highlights, two α-decay lines were observed in ^{251}Lr. Their properties indicate similar spins and parities for the ground state and the isomer as in ^{253}Lr. A new half-life value for the ^{253}Lr isomeric state was measured. A new branch from the $7/2^-$ isomer to the $11/2^-$ member of the $7/2^-$ band in ^{249}Md was proposed in ^{253}Lr. The Q_α values in Lr isotopes agree with the predictions of several mass models. The $7/2^-$ - $1/2^-$ level order in ^{251}Lr and ^{255}Lr was reproduced successfully in the cranked shell model with the particle-number-conserving method. These calculations underscored an important role of ε_6 hexacontetrapole deformation in the evolution of the single-proton energies in ^{251,253,255}Lr.

* seweryniak@anl.gov
† deceased

[1] Y. Oganessian and V. Utyonkov, Nucl. Phys. A **944**, 62 (2015).

[2] G. Münzenberg and K. Morita, Nucl. Phys. A **944**, 3 (2015).

[3] K. Morita, Nucl. Phys. A **944**, 30 (2015).

[4] Z. Y. Zhang, H. B. Yang, M. H. Huang, Z. G. Gan, C. X. Yuan, C. Qi, A. N. Andreyev, M. L. Liu, L. Ma, M. M. Zhang, Y. L. Tian, Y. S. Wang, J. G. Wang, C. L. Yang, G. S. Li, Y. H. Qiang, W. Q. Yang, R. F. Chen, H. B. Zhang, Z. W. Lu, X. X. Xu, L. M. Duan, H. R. Yang, W. X. Huang, Z. Liu, X. H. Zhou, Y. H. Zhang, H. S. Xu, N. Wang, H. B. Zhou, X. J. Wen, S. Huang, W. Hua, L. Zhu, X. Wang, Y. C. Mao, X. T. He, S. Y. Wang, W. Z. Xu, H. W. Li, Z. Z. Ren, and S. G. Zhou, Phys. Rev. Lett. **126**, 152502 (2021).

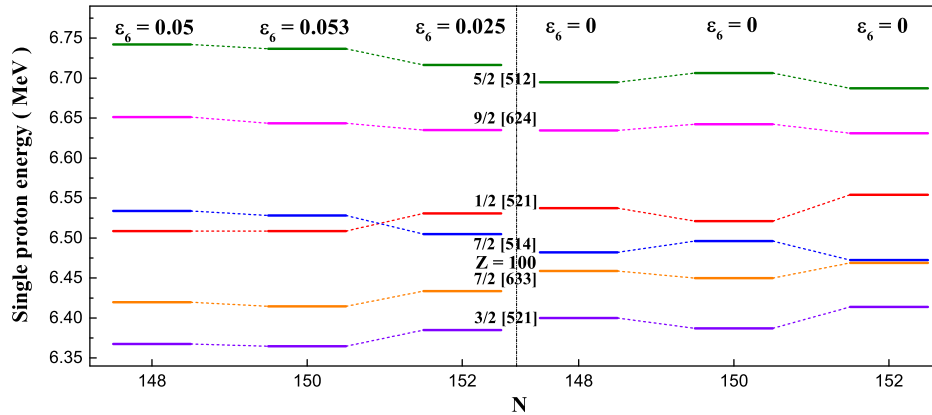[5] L. Ma, Z. Y. Zhang, Z. G. Gan, X. H. Zhou, H. B. Yang, M. H. Huang, C. L. Yang, M. M. Zhang, Y. L. Tian,

FIG. 6. Single-proton levels near the Fermi surface in ^{251,253,255}Lr calculated using the particle-number conserving cranked shell model [26]. The ε_6 values adopted in the calculation are indicated for each isotope.

Y. S. Wang, H. B. Zhou, X. T. He, Y. C. Mao, W. Hua, L. M. Duan, W. X. Huang, Z. Liu, X. X. Xu, Z. Z. Ren, S. G. Zhou, and H. S. Xu, Phys. Rev. Lett. **125**, 032502 (2020).

[6] J. Konki, J. Khuyagbaatar, J. Uusitalo, P. Greenlees, K. Auranen, H. Badran, M. Block, R. Briselet, D. Cox, M. Dasgupta, A. Di Nitto, C. Düllmann, T. Grahn, K. Hauschild, A. Herzán, R.-D. Herzberg, F. Heßberger, D. Hinde, R. Julin, S. Juutinen, E. Jäger, B. Kindler, J. Krier, M. Leino, B. Lommel, A. Lopez-Martens, D. Luong, M. Mallaburn, K. Nishio, J. Pakarinen, P. Papadakis, J. Partanen, P. Peura, P. Rahkila, K. Rezynkina, P. Ruotsalainen, M. Sandzelius, J. Sarén, C. Scholey, J. Sorri, S. Stolze, B. Sulignano, C. Theisen, A. Ward, A. Yakushev, and V. Yakusheva, Phys. Lett. B **764**, 265 (2017).

[7] J. L. Pore, J. M. Gates, R. Orford, C. M. Campbell, R. M. Clark, H. L. Crawford, N. E. Esker, P. Fallon, J. A. Gooding, J. T. Kwarsick, A. O. Macchiavelli, C. Morse, D. Rudolph, A. Såmark-Roth, C. Santamaria, R. S. Shah, and M. A. Stoyer, Phys. Rev. Lett. **124**, 252502 (2020).

[8] F. P. Heßberger, M. Block, C. E. Düllmann, A. Yakushev, M. Leino, and J. Uusitalo, Phys. Rev. Lett. **126**, 182501 (2021).

[9] I. Ahmad, A. M. Friedman, R. R. Chasman, and S. W. Yates, Phys. Rev. Lett. **39**, 12 (1977).

[10] A. Chatillon, C. Theisen, P. T. Greenlees, G. Auger, J. E. Bastin, E. Bouchez, B. Bouriquet, J. M. Casandjian, R. Cee, E. Clément, R. Dayras, G. de France, R. de Toureil, S. Eeckhaudt, A. Görgen, T. Grahn, S. Grévy, K. Hauschild, R. D. Herzberg, P. J. C. Ikin, G. D. Jones, P. Jones, R. Julin, S. Juutinen, H. Kettunen, A. Korichi, W. Korten, Y. Le Coz, M. Leino, A. Lopez-Martens, S. M. Lukyanov, Y. E. Penionzhkevich, J. Perkowski, A. Pritchard, P. Rahkila, M. Rejmund, J. Saren, C. Scholey, S. Siem, M. G. Saint-Laurent, C. Simenel, Y. G. Sobolev, C. Stodel, J. Uusitalo, A. Villari, M. Bender, P. Bonche, and P. H. Heenen, Eur. Phys. J. A **30**, 397 (2006).

[11] F. P. Heßberger, G. Münzenberg, S. Hofmann, Y. K. Agarwal, K. Poppensieker, W. Reisdorf, K. H. Schmidt,

J. R. H. Schneider, W. F. W. Schneider, H. J. Schött, P. Armbruster, B. Thuma, C. C. Sahm, and D. Vermeulen, Z. Phys. A **322**, 557 (1985).

[12] F. Heßberger, S. Hofmann, D. Ackermann, V. Ninov, M. Leino, G. Münzenberg, S. Saro, A. Lavrentev, A. Popeko, A. Yeremin, and C. Stodel, Eur. Phys. J. A **12**, 57 (2001).

[13] F. P. Heßberger, S. Hofmann, B. Streicher, B. Sulignano, S. Antalic, D. Ackermann, S. Heinz, B. Kindler, I. Kojouharov, P. Kuusiniemi, M. Leino, B. Lommel, R. Mann, A. G. Popeko, S. Šáro, J. Uusitalo, and A. V. Yeremin, Eur. Phys. J. A **41**, 145 (2009).

[14] F. P. Heßberger, S. Antalic, D. Ackermann, S. Heinz, S. Hofmann, J. Khuyagbaatar, B. Kindler, I. Kojouharov, B. Lommel, and R. Mann, Eur. Phys. J. A **43**, 175 (2010).

[15] A.-P. Leppanen, *Alpha-decay and decay-tagging studies of heavy elements using the RITU separator*, Ph.D. thesis (2005).

[16] F. P. Heßberger, S. Antalic, F. Giacoppo, B. Andel, D. Ackermann, M. Block, S. Heinz, J. Khuyagbaatar, I. Kojouharov, and M. Venhart, Eur. Phys. J. A **58**, 11 (2022).

[17] P. Brionnet, *Etude des états isomères des noyaux superlourds : cas des noyaux 257Db et 253 Lr*, Ph.D. thesis (2017).

[18] J. O. Rasmussen, Phys. Rev. **113**, 1593 (1959), publisher: American Physical Society.

[19] K. Hauschild, A. Lopez-Martens, A. V. Yeremin, O. Dorvaux, S. Antalic, A. V. Belozerov, C. Briancon, M. L. Chelnokov, V. I. Chepigin, D. Curien, B. Gall, A. Gorgen, V. A. Gorshkov, M. Guttormsen, F. Hanappe, A. P. Kabachenko, F. Khalfallah, A. C. Larsen, O. N. Malyshev, A. Minkova, A. G. Popeko, M. Rousseau, N. Rowley, S. Saro, A. V. Shutov, S. Siem, L. Stuttge, A. I. Svirikhin, N. U. H. Syed, C. Theisen, and M. Venhart, Phys. Rev. C **78**, 021302(R) (2008), publisher: American Physical Society.

[20] J. M. Gates, S. L. Nelson, K. E. Gregorich, I. Dragojevic, C. E. Dullmann, P. A. Ellison, C. M. Folden III, M. A. Garcia, L. Stavsetra, R. Sudowe, D. C. Hoffman, and H. Nitsche, Phys. Rev. C **78**, 034604 (2008), publisher:

American Physical Society.

[21] N. Wang, M. Liu, X. Wu, and J. Meng, Phys. Lett. B **734**, 215 (2014).

[22] P. Jachimowicz, M. Kowal, and J. Skalski, At. Data and Nucl. Data Tables **138**, 101393 (2021).

[23] P. Möller, A. Sierk, T. Ichikawa, and H. Sagawa, At. Data and Nucl. Data Tables **109-110**, 1 (2016).

[24] S. Goriely, N. Chamel, and J. M. Pearson, Phys. Rev. C **88**, 024308 (2013).

[25] S. Goriely, Nucl. Phys. A **933**, 68 (2015).

[26] X.-T. He, S.-Y. Zhao, Z.-H. Zhang, and Z.-Z. Ren, Chinese Phys. C **44**, 034106 (2020).

[27] A. Parkhomenko and A. Sobiczewski, Acta Phys. Pol. B **35**, 2447 (2004).

[28] G. G. Adamian, N. V. Antonenko, S. N. Kuklin, and W. Scheid, Phys. Rev. C **82**, 054304 (2010).

[29] N. Y. Shirikova, A. V. Sushkov, and R. V. Jolos, Phys. Rev. C **88**, 064319 (2013).

[30] H. L. Liu, F. R. Xu, P. M. Walker, and C. A. Bertulani, Phys. Rev. C **83**, 011303(R) (2011), publisher: American Physical Society.